Journal of Medicinal Chemistry

Article

pubs.acs.org/jmc

A New Strategy for Detection and Development of Tractable Telomerase Inhibitors

Elysia P. M. T. Cohn,[†] Kun-Liang Wu,[†] Thomas R. R. Pettus,*[,†] and Norbert O. Reich*[,†,‡]

[†]Department of Chemistry and Biochemistry, University of California, Santa Barbara, California 93106, United States

[‡]Program in Biomolecular Science and Engineering, University of California, Santa Barbara, California 93106, United States

Supporting Information

ABSTRACT: Despite intense academic and industrial efforts and innumerable in vitro and cell studies, no small-molecule telomerase inhibitors have emerged as drugs. Insufficient understanding of enzyme structure and mechanisms of interdiction coupled with the substantial complexities presented by its dimeric composition have stalled all progress toward small-molecule therapeutics. Here we challenge the assumption that human telomerase provides the best platform for inhibitor development by probing a monomeric *Tetrahymena* telomerase with six tool compounds. We find BIBR-1532 (**2**) and MST-312 (**5**) inhibit only human telomerase, whereas β-R (**1**), THyF (**3**), TMPyP4 (**6**), and EGCG (**4**) inhibit both enzymes. Our study demonstrates that some small-molecule scaffolds can be easily surveyed with in vitro studies using *Tetrahymena* telomerase, a finding that could lead to more tractable inhibitors with a greater potential for development given the more precise insights that can be gleaned from this more easily expressed and assayed monomeric enzyme.

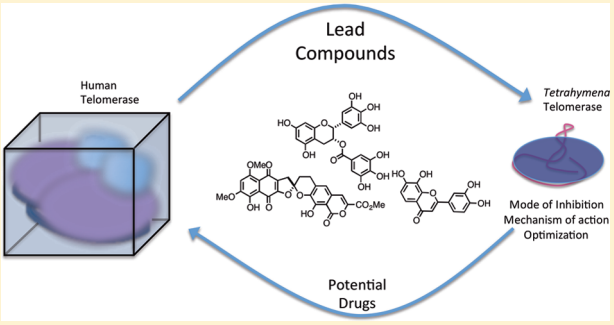

INTRODUCTION

Telomere length can determine genomic stability and cellular lifespan. The telomeres of normal somatic cells naturally shorten by 50−200 nucleotides with each cell cycle because of the inability to replicate the terminal bases on the lagging DNA strand.[1] Over time, telomeres reach a critically short length, resulting in genetic instability and subsequent apoptosis.[2] Immortal cells escape this telomere degradation mechanism by expressing telomerase, which extends short telomeres back to a stable length. The observed human telomerase (h-telomerase) activity in 80−95% of all cancers and absence from normal cells led to its subsequent validation as an anticancer target.[3]

Telomerase employs two mechanisms to extend the 3′-single-stranded ends of telomeres: a canonical nucleotide polymerization reaction, and a unique translocation step termed repeat addition processivity (RAP).[4] Its unique structure and mechanism provides an enticing target for the development of soluble small-molecule therapeutics, particularly given that its duties proceed almost entirely within the nucleus inside a cell.[5]

The customary strategy of building a complementary oligonucleotide that targets the template region has been successful and is well understood.[6] However, extensive investigations of small molecules over the past two decades have failed to yield structural understandings of their mechanisms for inhibiting h-telomerase.[7] One obstacle is the lack of sufficient quantities of stable and purified enzyme, which has thwarted access to a functionally relevant X-ray crystal structure.[8] In addition, h-telomerase serves as a functional dimer composed of two catalytic proteins (TERT), two integral RNAs (TER), and two dyskerin proteins, all of which complicates classical mechanistic studies.[8a] Moreover, many associated proteins (Hsp90, p23, POT1, TPP1, and TEP1) significantly affect the human enzyme's activity and processivity.[9] These issues have confounded traditional structure−function studies and will likely remain for the foreseeable future. Thus, it is not all together surprising that no small-molecule inhibitors have emerged from studies of the human enzyme.

Much of the structural and mechanistic understandings of h-telomerase have arisen from extrapolated studies of *Tetrahymena thermophila* telomerase (*t*-telomerase) because of its greater availability, easier expression, and monomeric composition.[10] The TERT components of human and *Tetrahymena* telomerases are similar in size (127 kD for human, 133 kD for *Tetrahymena*) and share sequence homology of 54% (21% identity) over the entire protein.[11] However, there is higher sequence identity in the catalytic reverse transcriptase (RT) domain, and both enzymes contain many other critical motifs including the TEN, TRBD, and CTE domains. The TER components of both enzymes also share many structural motifs despite the variation in size and differences in telomeric repeat sequence (5′-TT**G**GGG-3′ for *Tetrahymena* and 5′-TT**A**GGG-3′ for human). We therefore hypothesized that many of the structural components critical for catalytic activity would be conserved across the two enzymes, and we set out to interrogate both enzymes with several small molecule inhibitors in the hopes that the study of *Tetrahymena* could lead to more

Received: September 9, 2011
Published: March 13, 2012

dx.doi.org/10.1021/jm201191d | J. Med. Chem. 2012, 55, 3678−3686

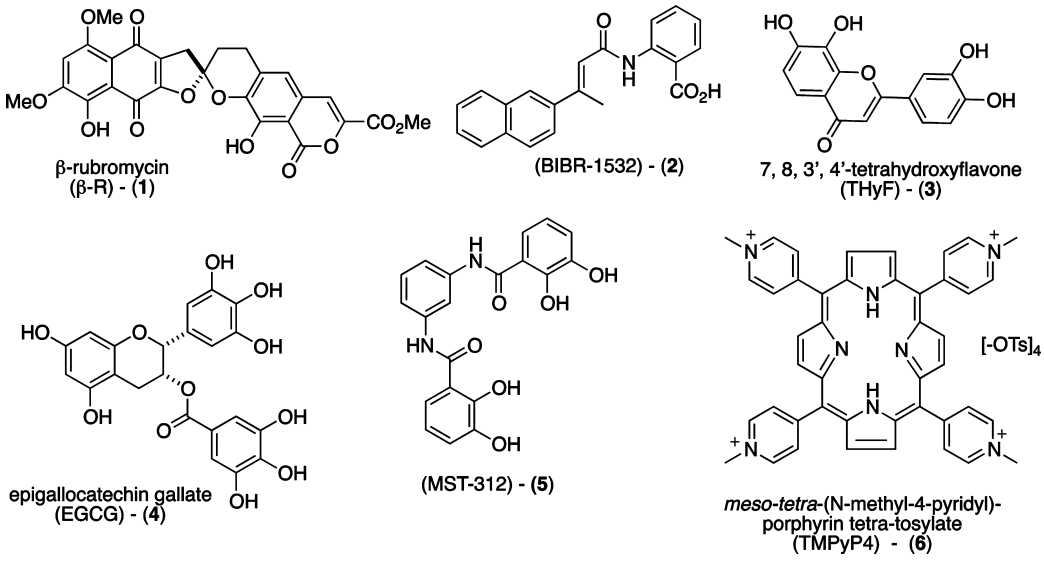

Figure 1. Known small-molecule h-telomerase inhibitors used as tool compounds for studies and comparisons.

detailed mechanistic understandings and tractable structure activity relationships than currently possible with the human enzyme.[12]

DESIGN AND PLAN

To accomplish this goal, we planned to use a panel of six well-known non-nucleoside h-telomerase inhibitors (**1**–**6**) to study the mechanistic similarities and differences between both telomerases (Figure 1). We would begin by rigorously validating our modified human TRAP (h-TRAP) assay with the previously reported telomerase inhibitors. The two-step telomeric repeat amplification protocol (TRAP) is the standard for rapidly interrogating inhibitors because it requires less enzyme and shorter times than the conventional ^{32}P-incorporation assay.[3] However, the original TRAP is prone to artifactual readings, particularly if the small molecule also inhibits the *Taq* DNA polymerase used in the amplification step.[13] Therefore, a purification step to remove these small molecules would be added. The potential for complications in the absence of such a step should give investigators pause when evaluating other telomerase studies. Not surprisingly, compounds **1**–**6** have afforded varying IC_{50} values throughout the literature (Table 1).[14] This variability reflects differing conditions and procedures. These factors obscure any direct comparisons from previous studies. We therefore needed a head-to-head assessment of both enzymes to rigorously guarantee our comparison. This premise mandated that we develop and deploy a new *t*-telomerase assay (*t*-TRAP) as a counterpart to h-TRAP in order to determine and compare potencies. This required that we redesign the DNA substrate and reverse PCR primer from the standard h-TRAP and substantiate catalytic activity in the new *t*-TRAP assay by the proper controls. Next, we would determine the mode of inhibition (MOI) for each inhibitor against each telomerase by deploying an efficient method using *two IC_{50}s to observe kinetics* (TIC-TOK). Finally, we would use the dissimilar inhibitor scaffolds to illuminate the similarities and differences between these two enzymes, with the intention of ultimately enabling refinements of those compounds that acted upon conserved components.

Table 1. Potencies of Compounds 1–6 for Human Telomerase[a]

Inhibitor	Raw h-TRAP IC_{50} (μM)	Spin h-TRAP IC_{50} (μM)	Literature Values (μM)
β-R (**1**)	1.32 ± 0.15	1.53 ± 0.21	3.0
BIBR-1532 (**2**)	3.6 ± 0.37	4.6 ± 0.48	0.093 – 20.0
THyF (**3**)	0.23 ± 0.01	0.25 ± 0.06	0.2 – 1.4
EGCG (**4**)	1.18 ± 0.16	1.08	1.0
MST-312 (**5**)	12.1 ± 0.9	12.8 ± 2.9	0.67
TMPyP4 (**6**)	0.06 ± 0.01	0.147 ± 0.02	0.22 – 10.0

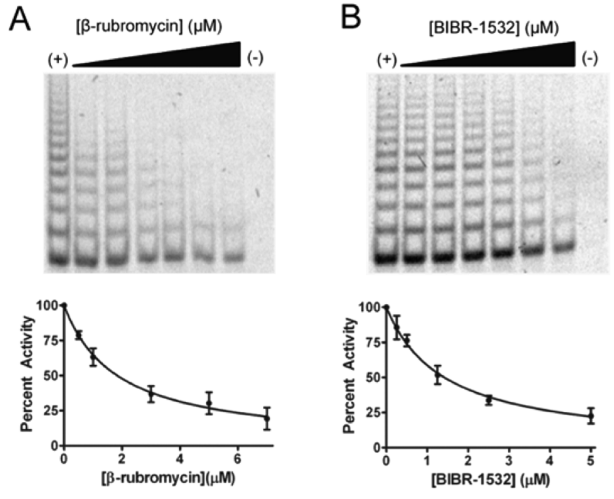

[a]h-TRAP assay readout of DNA products separated on 10% acrylamide gels and stained with SYBR Gold. Product formation decreases as inhibitor concentration increases from left to right. The density of DNA products in each lane is used to calculate the percent activity remaining. These values are then plotted as inhibitor concentration vs percent activity to extrapolate the IC_{50} values: *β*-rubromycin (A) and BIBR-1532 (B) gels with h-telomerase shown. Other graphs provided in Supporting Information.

RESULTS AND DISCUSSION

Using HeLa cell extracts as the source of h-telomerase, we re-evaluated compounds **1**–**6** in our h-TRAP assay and obtained

dx.doi.org/10.1021/jm201191d | J. Med. Chem. 2012, 55, 3678–3686

IC_{50} values that are generally in agreement with previously published values (Table 1).[14] β-R (**1**) displayed an IC_{50} of ~1.5 μM, which is close to Hayahi's published value of 3.06 ± 0.85 μM obtained using a modified TRAP assay. The small difference may be due to the variations in DNA substrate sequence and concentrations along with the use of K-562 (myelogenous leukemia) cell extract and a phenol/chloroform extraction step versus our Bio-Gel P6 spin column protocol for removal of the inhibitor before amplification.

For BIBR-1532 (**2**), we observed an IC_{50} of ~4.6 μM, which was significantly higher than the ~100 nM values previously reported by Damm et al. (2001) and Pascolo et al. (2002) but in the range of other more recently published values from TRAP assays (Table 1). Damm's and Pascolo's lower values most likely arise from their use of a ^{32}P-labeled nucleotide incorporation assay with purified telomerase.

THyF (**3**) displayed an IC_{50} of ~0.25 μM, which agreed with the value reported from a flash-plate assay that employed partially purified HEK293 (embryonic kidney) extracts (Table 1). Also, in agreement with previously reported literature values was the IC_{50} for EGCG (**4**) (~1.2 μM, Table 1). In contrast, MST-312 (**5**), a compound designed by Tsuruo et al. as a stable structural and functional analogue of EGCG (**4**), displayed an IC_{50} of ~12 μM in our hands. This value is greater (~18 times) than the published values (IC_{50} ~ 0.67–1.0 μM) obtained using telomerase isolated from U937 (histiocytic lymphoma) cell extracts. Our direct comparison of compounds **1**–**5** shows that the relative potencies are as follows: THyF (**3**) > EGCG (**4**) ≥ β-R (**1**) > BIBR-1532 (**2**) > MST-312 (**5**). To the best of our knowledge, this is the first such direct comparison of these small molecules on a level playing field.

TMPyP4 (**6**) and other G-quadruplex stabilizing ligands such as BRACO-19 and telomerstatin (both not shown) target the DNA product or the substrate, which folds into a G-quadruplex structure.[15] Furthermore, each stabilizing ligand binds specific G-quadruplex folds preferentially. These molecules also inhibit PCR by preventing primer annealing or sterically hindering *Taq* DNA polymerase from extending a dsDNA product. For this reason, the original TRAP assay is inappropriate for the characterization of G-quadruplex stabilizing molecules.[13,14i] It should be noted that with 27 cycles of amplification in a standard TRAP assay, a *Taq* inhibitor should have a multiplicative inhibitory effect. This could be addressed by adding a purification step between the extension reaction and PCR amplification. The application of various purification steps, such as phenol–chloroform extraction followed by ethanol precipitation,[14a] capture and purification of telomere extension products with a biotinylated telomere complement immobilized on streptavidin coated magnetic beads,[16] and QIA quick nucleotide purification kit (Qiagen)[13] might be sufficient to remove G-quadruplex inhibitors. However, we find that our Bio-Gel P6 spin column removes the vast majority of TMPyP4 but is most effective below 1.0 μM concentrations (Supporting Information). Thus, while TMPyP4 (**6**) inhibits the PCR amplification and telomerase with similar potencies (Table 2), our reported spin h-TRAP IC_{50} value of ~147 nM falls near the wide range of literature values, and we believe our value accurately reflects only h-telomerase inhibition (Table 1).

To confirm that none of the inhibitors were G-quadruplex stabilizing ligands, we performed thermal melt analyses (Figure 2). Only the presence of TMPyP4 (**6**) increased the melting temperature of the G-quadruplex structure. Therefore, inhibitors **1**–**5** are unlikely to inhibit through a G-quadruplex stabilizing mechanism or lead to artifactual potency overestimation.

Table 2. Measured Potencies of 1–6 for h-TRAP, *t*-TRAP, and PCR[a]

Inhibitor	h-TRAP IC_{50} (μM)	Maximal Inhibition	*t*-TRAP IC_{50}(μM)	Maximal inhibition	*Taq*-PCR IC_{50} (μM)
β-R (**1**)	1.53 ± 0.21	90%	0.81 ± 0.08	100%	54.6 ± 16.6
BIBR-1532 (**2**)	4.6 ± 0.48	100%	> 200	NA	> 60
THyF (**3**)	0.25 ± 0.06	100%	0.62 ± 0.17	100%	28.1 ± 8.5
EGCG (**4**)	1.18 ± 0.16	80%	0.37 ± 0.12	85%	> 75
MST-312 (**5**)	12.8 ± 2.9	100%	> 200	NA	> 60
$TMPyP_4$ (**6**)	0.15 ± 0.01	100%	0.14 ± 0.014	100%	0.15 ± 0.05

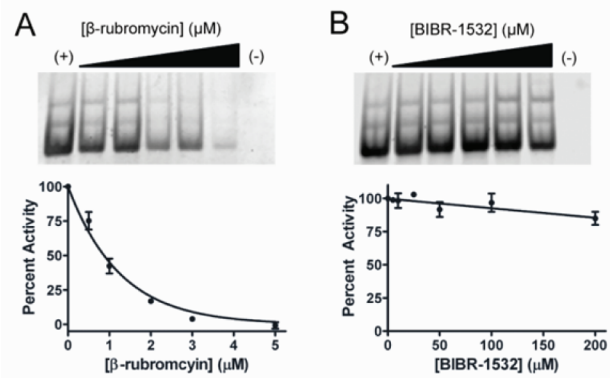

[a] *t*-TRAP assay DNA products separated on 10% acrylamide gels stained with SYBR Gold. Each lane shows the remaining activity as the inhibitor concentrations are increased from left to right. The product density in each lane is used to calculate the percent activity remaining and plotted against inhibitor concentration to determine the IC_{50} values. β-Rubromycin (A) and BIBR-1532 (B) gels with *t*-telomerase shown. Others graphs provided in Supporting Information.

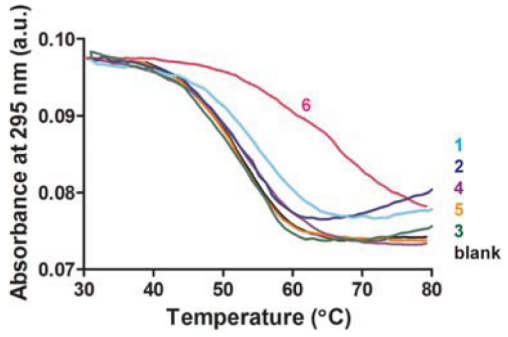

Figure 2. DNA G-quadruplex melting curve. Each line represents the melting of 2 μM TSG4 DNA in the presence or absence of inhibitors each at 2 μM: TMPyP4 (**6**), the red line is obviously skewed; others (**1**–**5**) are comparable to blank/black line.

t-TRAP Development. Our novel *t*-TRAP assay was formulated to be nearly identical with the h-TRAP assay, which requires a human telomerase substrate (h-TS) as well as a reverse primer for the PCR amplification. Our substrate for initiating the *t*-telomerase activity obviously had to be redesigned because of the different template region (3′-AACCCCAAC-5′ for *Tetrahymena* and 3′-AUCCCAAUC-5′ for human). However, we devised a dual functioning oligonucleotide that acted as the *t*-telomerase substrate (*t*-TS) and served as the forward primer in subsequent PCR amplification.[3] The 3′-end needed to

dx.doi.org/10.1021/jm201191d | J. Med. Chem. 2012, 55, 3678–3686

include three nucleotides so as to provide substrate recognition for the *t*-telomerase. On the other hand, the 5′-end could neither be telomeric nor a telomere complement but required a unique starting forward sequence. The *t*-TS sequence was modified to include the most commonly used 3′-end (5′-TTG-3′) for ^{32}P-incorporation assays with *t*-telomerase, whereas the 5′-end was adapted from the original h-TS to prevent unwanted formation of secondary structures and telomeric hybridization. These combined elements resulted in the development of the new 18-mer (5′-ACT TCG TAG AGC AGA TTG-3′) as the novel substrate for the *t*-TRAP assay.

In addition, we required the reverse primer for *Taq* DNA polymerase. This design of the sequence was predicated upon the h-ACX reverse primer employed in h-TRAP.[17] The h-ACX primer contains a 3′-end with one complete human telomeric repeat-complement followed by three additional telomeric repeat-complements containing a single A to T base switch. The 5′-region has a high G−C content and is neither telomeric nor a telomere complement. The 3′-region of the h-ACX functions to bind tandem telomeric repeats, and the 5′-region guides reverse primer annealing to the end of a single strand. Conserving these functions, we designed our *t*-telomerase reverse primer (*t*-ACX) with a single *Tetrahymena* telomeric repeat-complement on the 3′-end followed by two telomeric repeat-complements with a single C to T switch and the 6-nucleotide 5′-end with high G-C content that should not bind to a *Tetrahymena* telomere repeat or its complement. These combined elements resulted in the development of the new 24-mer (5′-GTG TGG CCA ATC CCA ATC CCA ACC-3′) as the novel reverse primer for the *t*-TRAP assay.

Our assay conditions also combined features from prior ^{32}P-incorporation studies of *t*-telomerase as well as TRAP studies using the human enzyme.[3,18] For the telomerase extension reactions, a buffer previously used by Collins was modified by exchanging *β*-me for DTT and adding EGTA. DTT is more stable and lowered the chances of inhibitor reduction. EGTA was meant to chelate any remaining Ca^{2+} from the starvation media. Unfortunately, the *Taq* DNA polymerase did not show optimal activity with this buffer. Therefore, 10 μL of extension reaction was diluted into 20 μL of 1× TRAP buffer with *t*-TS, *t*-ACX, and dNTPs. In this manner, both enzymes exhibited optimal activity without complete buffer exchange. We decided to use the Bio-Gel P6 spin column purification step with only TMPyP4 (**6**) because the other inhibitors (**1**−**5**) failed to interact appreciably with T*aq* and 3-fold dilution prior to PCR would result in very low compound concentration. For example, EGCG (**4**) had an IC_{50} value of ∼28 μM in PCR (*Taq*-PCR, Table 2), yet the highest EGCG (**4**) concentration assayed in *t*-TRAP was 10 μM, which was further diluted to 3.3 μM before PCR. Thus, the concentration of EGCG (**4**) present during amplification is significantly lower (∼10 times) than the IC_{50} for PCR amplification.

It should be noted that the *t*-TRAP assay, like the popular h-TRAP assay, has a few shortcomings. First, TRAP assays only measure total telomerase activity. These assays cannot be used to study single nucleotide addition, processivity, or RAP. Second, a DNA polymerase inhibitor will show a false positive for telomerase inhibition in a TRAP assay unless removed prior to the PCR amplification. It is important to know the limitations of an assay to properly deploy them and accurately access the results.

Using our *t*-TRAP assay, we determined the IC_{50} values of compounds **1**−**6** (*t*-TRAP, Table 2). Four of the six compounds previously designated as h-telomerase inhibitors also inhibited *t*-telomerase. Neither BIBR-1532 (**3**) nor MST-312 (**5**) inhibited *t*-telomerase at concentrations of up to 200 μM. These compounds previously displayed IC_{50} values of 4.6 ± 0.48 μM and 12.8 ± 2.9 μM for h-telomerase in our hands (h-TRAP, Table 2). It is remarkable that BIBR-1532 (**2**), perhaps the best characterized and broadly used standard for in vitro inhibition of h-telomerase, showed *no effect* on *t*-telomerase. It has been proposed that BIBR-1532 (**2**) inhibits h-telomerase by interfering with its RAP, which is a mechanism unique to telomerases.[14i] The distinctions we observed across the two enzymes clearly suggest that the RAP mechanisms for these two telomerases are different.

Inhibition of *t*-telomerase by TMPyP4 (**6**) was anticipated because the cyclic porphyrin is well-known as a potent but nonselective G-quadruplex stabilizing ligand.[19] In this manner, TMPyP4 (**6**) served as a positive control confirming our ability to properly report inhibition. While it has been reported that compound **6** can associate with both human and *Tetrahymena* telomere constructed G-quadruplex structures and prevent further extension, some evidence supports additional non-DNA-sequestering mechanisms.[14i] Irrespective of its role, the IC_{50} value obtained for *t*-telomerase (0.14 ± 0.03 μM) was almost identical to those obtained for h-telomerase (Table 2).

β-R (**1**), THyF (**3**), and EGCG (**4**) also efficiently inhibited *t*-telomerase. *β*-R (**1**) was about twice as effective for *t*-telomerase as for h-telomerase, and it achieved 100% maximal inhibition. THyF (**3**) also achieved 100% maximal inhibition for both telomerases but was 3-fold more potent against h-telomerase. EGCG (**4**) displayed three times greater potency toward *t*-telomerase and similar maximal inhibition (∼80%) against both enzymes (Figure 3).

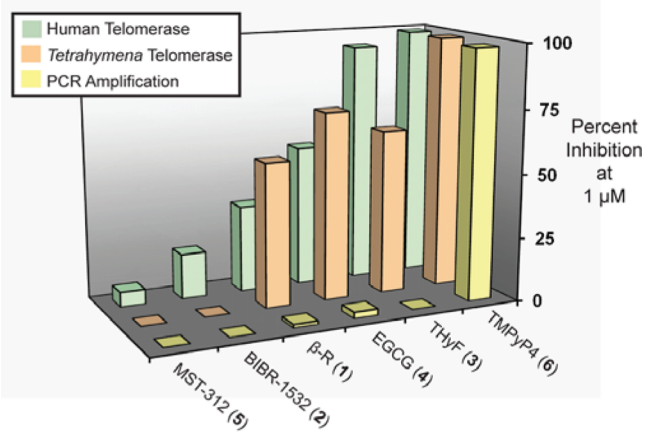

Figure 3. Another way to view the relative inhibition of h-telomerase, *t*-telomerase, and PCR amplification by the six tool compounds.

Mode of Inhibition. We next sought to determine if the comparable potencies resulted from a similar MOI. We began by determining the substrate K_m values for the respective DNA substrates, (10.8 ± 1.5 nM h-TS for h-telomerase and 22.9 ± 4.1 nM *t*-TS of *t*-telomerase), and for dNTPs, (14.0 ± 2.6 μM for h-telomerase and 0.83 ± 0.10 nM for *t*-telomerase) (Supporting Information). Unfortunately, the sensitivity of each TRAP assay using substrate (TS and dNTP) concentrations below the K_m resulted in insignificant signal and prevented traditional analyses.

dx.doi.org/10.1021/jm201191d | *J. Med. Chem.* 2012, 55, 3678−3686

We therefore developed an alternative method not requiring data collection below K_m. By modeling simple forms of inhibition (competitive, noncompetitive, mixed-type, and uncompetitive), we found the ratio of high substrate concentration ($[S_H]$) to the K_m concentration is proportional to the ratio of the IC_{50} values determined at those concentrations (see Supporting Information). The relationship between these two ratios is different for each MOI (Figure 4). This method, which we

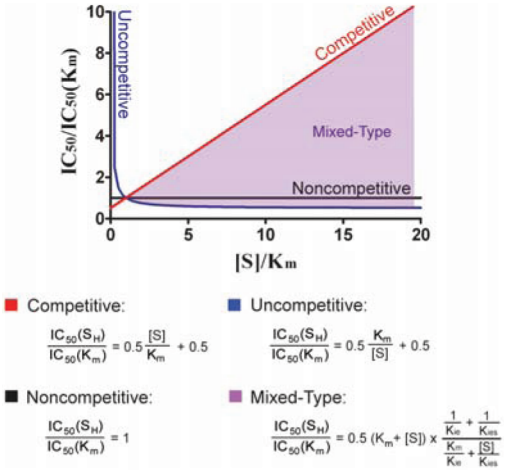

Figure 4. TIC-TOK MOI analysis. Graph showing the use of two IC_{50} values to obtain kinetics for establishing MOI by computing the IC_{50} ratios from two substrate concentrations $[S]$ and K_m. $IC_{50}(S_H) = IC_{50}$ value attained at high $[S]$, whereas $IC_{50}(K_m) = IC_{50}$ values attained at a substrate concentration equal to the K_m. Each MOI displays a unique relationship between IC_{50} ratio values and the $[S]/K_m$ as shown by the equations above. For mixed-type, K_{ie} is the equilibrium constant for E + I ↔ EI and K_{ies} is the equilibrium constant for ES + I ↔ ESI.

have termed **T**wo **IC**$_{50s}$ **T**O **O**bserve **K**inetics (TIC-TOK) can efficiently and qualitatively assign a MOI to a compound. We have subsequently learned that a similar method using EC_{50}s in high throughput analyses was previously reported by Wei et al.[20]

To confirm that the application of TIC-TOK with a TRAP assay can accurately report these relationships between substrate concentrations and IC_{50} values, we tested BIBR-1532 (**2**) against h-telomerase because its mechanism had been described.[14i] From the inhibition curves we obtained at high substrate ($[S_H]$ > 9-fold K_m) and K_m substrate concentrations, we determined the IC_{50} ratios, thereby providing the basis for distinguishing between MOIs. The IC_{50} values for BIBR-1532 (**2**) for h-telomerase were essentially unchanged between $[S_H]$ and K_m substrate concentration (IC_{50} ratios of ~1), which is consistent with BIBR-1532 (**2**) being a noncompetitive inhibitor with respect to h-TS and dNTPs (Figure 5). Furthermore, these IC_{50} ratios are slightly greater than 1, suggesting some mixed-type character to the MOIs. This finding agrees with previously published data. A similar analysis of *β*-R (**1**), EGCG (**4**), and THyF (**3**) was also carried out for both human and *Tetrahymena* telomerases. The substrate concentrations from the prior BIBR-1532 (**2**) study were again used for the h-telomerase MOI studies. *t*-Telomerase studies used analogous low and high substrate concentrations. From these, the ratios of IC_{50} values that should be obtained for each MOI for each telomerase were calculated (Table 3). These predicted IC_{50} ratios were then compared to the observed IC_{50} ratios to

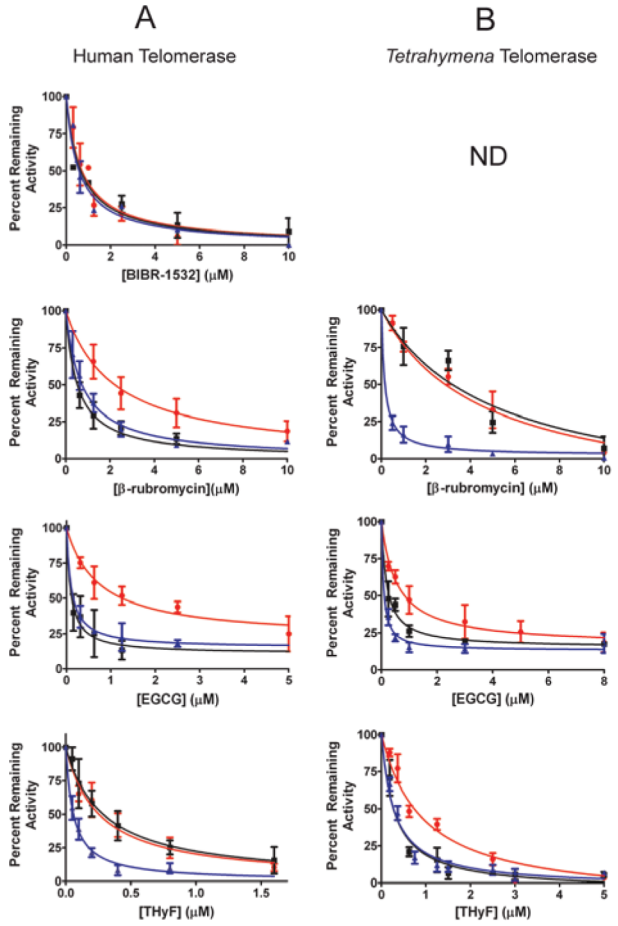

Figure 5. TIC-TOK MOI analysis of inhibitors with regards to both telomerases. Each curve represents the inhibition observed under three conditions: high [TS] and high [dNTPs] (red), [TS] = K_m and high [dNTPs] (blue), and high [TS] and [dNTPs] = K_m (black).

Table 3. Substrate Concentrations Used in the TIC-TOK MOI Analyses (top), and Calculated/Predicted IC_{50} Ratios for Each MOI with Respect to Each Substrate for Each Telomerase (Directly Below)

Telomerase	TS			dNTPs		
	K_m (nM)	$[S_H]$ (nM)	$[S_H]/K_m$	K_m (μM)	$[S_H]$(μM)	$[S_H]/K_m$
Human	10	360	36	14	130	9.3
tetrahymena	20	360	18	0.8	40	50

Predicted MOI	h-telomerase $IC_{50}(S_H)/IC_{50}(K_m)$		*t*-telomerase $IC_{50}(S_H)/IC_{50}(K_m)$	
	h-TS	dNTPs	*t*-TS	dNTPs
Competitive	18.5	5.1	9.5	25.5
Noncompetitive	1	1	1	1
Uncompetitive	0.51	0.55	0.53	0.51
Mixed Type	0.51 < x < 18.5	0.55 < x < 5.1	0.53 < x < 9.5	0.51 < x < 25.5

qualitatively determine the MOI for each compound with respect to the corresponding TS and dNTPs (Table 4).

For h-telomerase, we determined that *β*-R (**1**), EGCG (**4**), and THyF (**3**), were mixed-type inhibitors with respect to h-TS, having IC_{50} ratios of 3.03 ± 0.73, 8.16 ± 3.05, and 4.30 ± 0.26, respectively (Table 4), which fall between 0.51 and 18.5 as

dx.doi.org/10.1021/jm201191d | J. Med. Chem. 2012, 55, 3678–3686

Table 4. Measured IC_{50} Ratios and Qualitative MOI Assignment for Inhibitors with Regards to Both TS and dNTP in Each Telomerase

Inhibitor	h-telomerase $IC_{50}(S_H)/IC_{50}(K_m)$		*t*-telomerase $IC_{50}(S_H)/IC_{50}(K_m)$	
	h-TS	dNTPs	*t*-TS	dNTPs
β-R (**1**)	3.03 ± 0.73 Mixed Type	4.22 ± 0.97 Mixed Type	17.9 ± 1.1 Competitive	0.90 ± 0.01 Noncompetitive
EGCG (**4**)	8.16 ± 3.05 Mixed Type	10.56 ± 4.77 Competitive	8.33 ± 1.50 Competitive	3.02 ± 0.62 Mixed Type
THyF (**3**)	4.30 ± 0.86 Mixed Type	0.89 ± 0.21 Noncompetitive	2.71 ± 0.24 Mixed Type	2.75 ± 0.29 Mixed Type
BIBR-1532 (**2**)	1.21 ± 0.26 Noncompetitive	1.07 ± 0.29 Noncompetitive	NA	NA

was expected for mixed-type inhibitors of h-telomerase (Table 3). In contrast, each inhibitor had a different MOI with respect to dNTPs. β-R (**1**) was mixed-type with an IC_{50} ratio of 4.22 ± 0.97, which is between 0.55 and 5.1 but within error of the expected IC_{50} ratio of 5.1 for a competitive inhibitor, which suggests a strong competitive nature (Table 4). EGCG (**4**) was competitive with an IC_{50} ratio of 10.56 ± 4.77, which is higher than the predicted IC_{50} ratio of 5.1 but still within the large associated error. THyF (**3**) was noncompetitive with an IC_{50} ratio of 0.89 ± 0.21, which is very close to the expected noncompetitive ratio of 1 (Table 3). The competitive nature of β-R (**1**) and EGCG (**4**) with respect to the DNA substrate agrees with previously published data. Furthermore, the mixed-type MOI of β-R (**1**) with respect to dNTPs also agrees with the literature. To the best of our knowledge, there has been no MOI published for THyF (**3**) with respect to either h-TS or dNTP binding or for EGCG (**4**) with respect to dNTP binding.

For *t*-telomerase, we determined β-R (**1**) and EGCG (**4**) were both competitive with respect to *t*-TS, having IC_{50} ratios of 17.9 ± 1.1 and 8.3 ± 1.5, respectively (Figure 5). Oddly, the IC_{50} ratio of β-R (**1**) is about twice the estimated ratio of 9.5 for a competitive inhibitor which may result from its $IC_{50}(K_m)$ value being close to the lower detection limit of the assay. In contrast, THyF (**3**) was determined to be a mixed-type inhibitor with respect to *t*-TS with an IC_{50} ratio of 2.71 ± 0.24, which falls between 0.53 and 9.5 as expected (Table 3). The MOIs with respect to dNTPs were determined to be mixed-type for EGCG (**4**) and THyF (**3**) with IC_{50} ratios of 3.02 ± 0.62 and 2.75 ± 0.29, which fall between 0.51 and 25.5 as expected, and β-R (**1**) was found to be noncompetitive with an IC_{50} ratio of 0.9 ± 0.01, which is very close to the expected value of 1 (Table 4).

As a dimeric enzyme, h-telomerase may show non-Michaelis–Menten kinetics due to cooperativity between two active sites on a homodimer. In this regard, only a noncompetitive assignment of a MOI can be concluded as accurate. Assignments of other MOIs are more ambiguous and would require additional information to draw meaningful conclusions. In contrast, monomeric *t*-telomerase should display Michaelis–Menten kinetics, making the MOI analysis more robust for this enzyme. Dual analysis of MOI data from both enzymes will yield more meaningful conclusions about h-telomerase inhibition than can be deduced by analysis of human alone.

Our MOI analyses have shown that THyF (**3**) inhibits both human and *Tetrahymena* telomerases in a similar manner. THyF (**3**) is a mixed-type inhibitor of both enzymes with respect to the TS. The MOIs with respect to dNTPs are pure noncompetitive for h-telomerase and mixed-type leaning toward noncompetitive (as determined by the IC_{50} ratio proximity to the predicted noncompetitive value) for *t*-telomerase. This suggests that THyF (**3**) can inhibit both enzymes without interfering with dNTP binding in either.

β-R (**1**) and EGCG (**4**) exhibit different MOIs against each telomerases with respect to TS and dNTPs. However, the likelihood that an inhibitor affects two supposedly homologous enzymes by interacting with different domains of each enzyme seems intuitively far-fetched. No patterns can be deciphered from the MOIs of either compound with respect to dNTPs. However, there is a recognizable trend across the two enzymes with respect to the DNA substrates. Both β-R (**1**) and EGCG (**4**) show mixed-type kinetics with respect to h-TS and competitive kinetics with respect to *t*-TS. This consistent trend might be explained by the dimeric state of h-telomerase versus the monomeric state of *t*-telomerase. Multimeric enzymes with more than one functional active site show *non*-Michaelis–Menten kinetics due to cooperativity between their active sites,[21] therefore their MOIs are often misinterpreted.[22] h-Telomerase is a homodimer, and evidence suggests that both are functional and possibly regulated by DNA substrate binding.[23] The modulation of one active site could increase the substrate affinity at the other or alter the rate of catalysis.[22] Therefore, regulation in a dimeric enzyme would result in a decrease in the effective K_m. In such a case, a competitive inhibitor would appear by MOI analysis as mixed-type because the substrate binding affinity of the remaining sites is increased. If there were no communication between active sites, or the enzyme was a monomer, then the inhibitor would appear to be purely competitive. Therefore, the observation of mixed-type inhibition for dimeric h-telomerase and competitive inhibition for monomeric *t*-telomerase by β-R (**1**) and EGCG (**4**) supports the theory that these molecules interact with analogous component(s) on each enzyme but display different MOIs due to the difference in respective multimeric state.

CONCLUSIONS

We have produced standardized inhibition data for six well-known albeit structurally and mechanistically distinct telomerase inhibitors through careful and thorough studies with the human enzyme using a modified TRAP assay that improves the accuracy of IC_{50} measurements. We have developed and validated a new *t*-TRAP assay and then applied this to the same six inhibitors. Next, we have established and deployed a new rapid method (TIC-TOK), which enabled us to determine the modes of inhibition (competitive, noncompetitive, uncompetitive, mixed-type) by two straightforward IC_{50} measurements at two substrate concentrations. Our subsequent study of these six tool compounds across the two enzymes has revealed several mechanistic insights.

Four of the six compounds tested inhibited both enzymes, implying structural and mechanistic overlap between the two telomerases. Our further kinetic comparison of THyF (**3**) inhibition of human and *Tetrahymena* telomerases suggests a similar mode of inhibition showing structural and/or mechanistic conservations excluding dNTP binding. Analysis of β-R (**1**) and EGCG (**4**) inhibition with both enzymes supports the existence of cooperativity between the DNA substrate binding sites of dimeric h-telomerase, which would make an otherwise competitive inhibitor appear to have mixed-type kinetics. In contrast, BIBR-1532 (**2**), which is believed to inhibit the translocation step of h-telomerase, did not inhibit *t*-telomerase,

dx.doi.org/10.1021/jm201191d | J. Med. Chem. 2012, 55, 3678–3686

suggesting that the two enzymes may have distinct translocation (RAP) mechanisms.

This study confirms that some classes of telomerase inhibitors can be studied with the readily available, easily cultured, and more robust *Tetrahymena* enzyme with the anticipation that the findings will be relevant and comparable with h-telomerase. Because four of six compounds inhibit both enzymes, our work indicates that the two telomerases are structurally similar, despite their difference in multimeric states and TER components. Our tool compounds also show that there are some important and perhaps unrecognized functional distinctions between RAP and dNTP binding for the two enzymes. Taking these observations into consideration, it is evident that these should not be targeted when using *t*-telomerase to detect and develop new inhibitors. While we acknowledge that sorting telomerase inhibitors by *t*-telomerase will result in some h-telomerase scaffolds being missed, we consider this a small loss given the potential for first rational improvements within those scaffolds that are identified.

t-Telomerase could be useful for detecting and developing small molecules, which would be competitive with respect to the DNA substrate, possibly through some conserved interaction. Our data implies that β-R (**1**) and EGCG (**4**) act as competitive inhibitors of *t*-telomerase and can be structurally optimized using *Tetrahymena* to yield more potent h-telomerase inhibitors. We therefore agree with Hayashi[14a] that the spiroketal scaffold of β-R (**1**) provides the best lead inhibitor, as EGCG (**4**) is well-known to be very promiscuous, and both EGCG (**4**) and THyF (**3**) are chemically unstable. Thus, *t*-TRAP assays can, in principle lead to the identification of future inhibitors whose structural targets can be more easily and specifically identified in the monomeric *t*-telomerase. Once the site and specific atomic mechanism of interdiction has been established in future studies, then this knowledge would make identification of the analogous site in the human enzyme more straightforward.

EXPERIMENTAL SECTION

h-TRAP. TRAP was preformed as described previously with some modifications.[3,17] Reactions were run in TRAP buffer (20 mM Tris-HCl pH 8.0, 68 mM KCl, 1.5 mM $MgCl_2$, 1 mM EGTA pH 8.0, 100 μg/mL BSA, 0.05% Tween 20), 50 μM dNTPs, and 100 ng h-TS (5′-AAT CCG TCG AGC AGA GTT-3′). HeLa cell extracts were diluted into CHAPS lysis buffer before being added to reaction mix. TRAP buffer, extracts, and inhibitors (dissolved in DMSO) were incubated on ice for 15 min prior to extension reaction initiation by addition of h-TS and dNTPs. Total reaction volumes were 50 μL performed at 25 °C for 10 min, followed by 90 °C for 5 min. When necessary, extension products were purified through a Bio-Gel P6 spin column (50 μL loaded onto a 1 mL P6-gel bed) and transferred to new PCR tubes before adding 100 ng h-ACX (3′-GCG CGG CTT ACC CTT ACC CTT ACC CTA ACC-5′), 2.5 nmol dNTPs, and 2 units *Taq*. If no purification column was preformed, only h-ACX primer and *Taq* were added directly to each completed extension reaction. PCR reactions were 27 cycles of: 95 °C for 30s, 50 °C for 30s, 72 °C for 60s. PCR products were separated by 10% (19:1) PAGE at 350 V for 1.5 h, stained with SYBR gold, visualized on a Storm 840 or Typhoon Trio, and densitometry was preformed on Image Quant5 or ImageQuantL. At least one of the three (or more) experiments was preformed on a different day from the others, introducing some interexperiment variability. Experiments conducted on the same day used separate master mixes and separate enzyme aliquots.

Bio-Gel P6 Spin Column Purification.[14iii] Bio-Gel P6 Gel, medium, (Bio-Rad) was pre-equilibrated in 1× TTRB for *t*-TRAP or in 1× TRAP buffer for h-TRAP (1.2 g dry gel to 10 mL) for at least 24 h at 4 °C. P6-gel columns were assembled and prepared by loading 1 mL of equilibrated P6-gel into a Bio-Spin disposable chromatography column (Bio-Rad). The equilibration buffer was removed by centrifuging columns twice at 2000 rpm for 2 min in a Centra CL2 ThremoIEC. Between spins the flow through was discarded. Columns were then transferred to new 1.5 mL Eppendorf tubes before extension reaction products were loaded onto the P6-gel. Extension reaction products were spun down at 2000 rpm for 2:30 min, and purified products were used in the following PCR reactions.

PCR Inhibition. To measure the effects of each inhibitor on PCR amplification, the h-TRAP assay was performed with the addition of inhibitor after the extension reaction. These products were separated on an acrylamide gel and analyzed as previously described for h-TRAP.

***t*-TRAP.** Extension reactions were run in TTRB (50 mM Tris-HCl pH 8.0, 10 mM spermidine, 2 mM DTT, 2 mM $MgCl_2$, 1 mM EGTA pH 8.0). Buffer, cell extracts (diluted into TLB), and inhibitors (dissolved in 1:1 DMSO:H_2O) were incubated on ice for 10 min prior to initiation of the extension reaction by addition of *t*-TS (3′-ACT TCG TAG AGC AGA TTG-5′) and dNTPs to final concentrations of 40 nM and 50 μM, respectively. Total extension reaction volumes were 25 μL and were run at 30 °C for 15 min, followed by a heat kill step (90 °C for 5 min). When testing the potency of inhibitors, which also affect *Taq*, extension products were purified through a Bio-Gel P6 spin column (20 μL of reaction volume loaded onto a 1 mL P6-gel bed). Then 10 μL of purified or unpurified extension product was then added to 20 μL of PCR mix: 1× TRAP buffer, 50 ng *t*-TS, 50 ng *t*-ACX (5′- GTG TGG CCA ATC CCA ATC CCA ACC-3′), 75 μM dNTPs, and 2 units *Taq*. PCR reactions were 26 cycles of: 95 °C for 30s, 60 °C for 30s, 72 °C for 45s. PCR products were separated by 10% (19:1) PAGE at 350 V for 1.5 h, stained with SYBR Gold, visualized on a Typhoon Trio (488 nm (blue) excitation, 526 nm emission filter), and densitometry was performed using ImageQuantLT software. Replicate experiments were preformed in the same manner as in the h-TRAP.

Note: *t*-TRAP, much like h-TRAP requires a high degree of care as results can be affected by RNase and DNA contamination. Because no RNase inhibitors were used in this study, we suggest making all buffers and reagent dilutions with sterile DEPC treated water. To avoid DNA contamination, we suggest changing gloves often, making small aliquots of all reagents, occasionally bleaching Eppendorf and PCR tube racks, and handling final *t*-TRAP products on a separate surface from that at which the assays are preformed.

Mechanism of Inhibition Analysis. The previously described h-TRAP and *t*-TRAP assays were preformed in triplicate using high/saturating concentrations of substrate and substrate concentrations equal to the K_m. The h-TRAP assay was preformed under three different conditions: (1) 360 nM TS and 130 μM dNTPs, (2) 360 nM TS and 14 μM dNTPs, and (3) 10 nM TS and 130 μM dNTPs. For the *t*-telomerase studies, analogous conditions were used: (1) 360 nM *t*-TS and 40 μM dNTPs, (2) 360 nM *t*-TS and 0.8 μM dNTPs, and (3) 20 nM *t*-TS and 40 μM dNTPs. The IC_{50} values where extrapolated from product densities and the IC_{50} ratios were compared to predicted ratios.

Inhibitor Procurement. TMPyP4 (**6**) was purchased from Frontier Scientific. 7,8,3′,4′-Tetrahydroxyflavone (**3**) was purchased from Indofine Chemical Company, Inc. EGCG (**4**) was purchased from Alexis Biochemicals, and β-rubromycin (**1**) was purchased from Enzo Life Sciences. BIBR-1532 (**2**) was synthesized according to literature procedure.[12] MST-312 (**5**) was both synthesized[14i] and purchased from Sigma-Aldrich. All synthesized compounds were clean by ^{1}H NMR (>95%). Purchased compounds were assumed to have >95% purity based upon information provided by the commercial vendor.

DNA Quadruplex Melting Curves. Melting curves were preformed on a Beckman Counter DU 800 spectrophotometer. Each sample included 20 mM Tris-HCl pH 8.0, 68 mM KCl, 1.5 mM $MgCl_2$, 2 μM TSG4 (5′-$(GGGATT)_3$GGGTT-3′), and 2 μM of inhibitor. All inhibitors were dissolved in a 1:1 DMSO:H_2O solution, and then added to the TSG4 sample. Samples were ramped up from 30 to 82 °C at 0.5 °C per min, and 295 nm absorbance values were sampled every 30 s. Samples were then ramped down from 82 to 30 °C in the same manner to confirm reversibility of the quadruplex melting process in the presence and absence of inhibitors.

■ ASSOCIATED CONTENT

Supporting Information

Cell culture procedures, *t*-TRAP assay controls, additional inhibition curves, Bio-Gel P6 spin column studies, TRAP assay Michaelis–Menten curves, IC_{50} values obtained from TICTOK analyses, and explanation of method. This material is available free of charge via the Internet at http://pubs.acs.org.

■ AUTHOR INFORMATION

Corresponding Author

*For T.R.R.P.: phone, 805-637-5651; e-mail, pettus@chem.ucsb.edu. For N.O.R.: phone, 805-893-8368; e-mail, reich@chem.ucsb.edu.

Notes

The authors declare no competing financial interest.

■ ACKNOWLEDGMENTS

T. R. R. Pettus acknowledges support of rubromycin synthetic efforts by the National Science Foundation through an Early Career Award (0135031) and a regular NSF Award (CHE-0806356). K.-L. Wu is appreciative of a dissertation fellowship granted by the University of California Tobacco-Related Disease Research Program (TRDRP) as well as for departmental support provided as B. R. Baker Fellowship Fund for excellence in biologically related chemistries established by Reba Baker to commemorate Professor B. R. Baker's formative role at UCSB. We thank Ed Orias (UCSB) for the *Tetrahymena thermophila* strain and his helpful advice. We also thank all reviewers and editors for their important efforts and helpful criticisms.

■ ABBREVIATIONS USED

ssDNA, single-stranded DNA; dsDNA, double-stranded DNA; dNTPs, deoxynucleotide triphosphates; PCR, polymerase chain reaction; TERT, telomerase reverse transcriptase; TER, internal telomerase RNA; TEN, essential N-terminal domain of telomerase; TRBD, telomerase RNA binding domain; RT, reverse transcriptase; CET, C-terminal domain of telomerase; POT1, protection of telomeres protein 1; TPP1, telomere protecting protein and (binding partner to POT1); TEP1, telomerase-associated protein 1; Hsp90, heat shock protein 90; p23, molecular chaperon protein 23; RAP, repeat addition processivity; MOI, mode of inhibition; DEPC, diethyl pyrocarbonate; β-me, β-mercaptoenthanol; DTT, dithiothreitol; Tris, tris(hydroxymethyl)aminomethane; EGTA, ethylene glycol tetraacetic acid; EDTA, ethylene diamine tetraacetic acid; h-TRAP, human telomeric repeat amplification protocol; *t*-TRAP, *Tetrahymena* telomeric repeat amplification protocol; h-TS, human telomerase substrate; h-ACX, reverse primer for h-TRAP; *t*-TS, *Tetrahymena* telomerase substrate; *t*-ACX, reverse primer for *t*-TRAP; TTRB, *Tetrahymena* telomerase reaction buffer; TMPyP4, *meso*-tetra (*N*-methyl-4-pyridyl) porphine tetratosylate (**6**); EGCG, epigallocatechin-3-gallate (**4**); THyF, 7,8,3′,4′-tetrahydroxyflavone (**3**); β-R, β-rubromycin (**1**); BIBR-1532 (**2**), 2-((*E*)-3-naphthalene-2-yl-but-2-enoylamino)-benzoic acid; MST-312 (**5**), *N*,*N*-1,3-phenylenebis-(2,3-dihydroxy-benzamide); *Taq*, *Thermus aquaticus* DNA polymerase; CHAPS, 3[(3-cholamidopropyl)dimethylammonio]-propanesulfonic acid; TLB, *Tetrahymena* lysis buffer

■ REFERENCES

(1) Hiyama, K.; Hiyama, E.; Shay, J. W. Telomeres and Telomerase in Humans. In *Telomeres and Telomerase in Cancer*, Series: Cancer Drug Discovery and Development; Hiyama, K., Ed.; Springer Press: New York, 2009; pp 3–21.

(2) Stewart, S. A.; Weingerg, R. A. Telomeres: Cancer to Human Aging. *Annu. Rev. Cell Dev. Biol.* **2006**, *22*, 531–557.

(3) Piatyszek, M. A.; Kim, N. W.; Weinrich, S. L.; Hiyama, K.; Hiyama, E.; Wright, W. E.; Shay, J. W. Detection of telomerase activity in human cells and tumors by a telomeric repeat amplification protocol (TRAP). *Methods Cell Sci.* **1995**, *17*, 1–15.

(4) Blackburn, E. H.; Collins, K. Telomerase: An RNP Enzyme Synthesizes DNA. *Cold Spring Harbor Perspect. Biol.* **2011**, *3*, a003558.

(5) (a) Etheridge, K. T.; Banik, S. S. R.; Armbruster, B. N.; Zhu, Y.; Terns, R. M.; Terns, M. P.; Counter, C. M. The Nucleolar Localization Domain of the Catalytic Subunit of Human Telomerase. *J. Biol. Chem.* **2002**, *277*, 24764–24770. (b) Imai, K.; Takaoka, A. Comparing antibody and small-molecule therapies for cancer. *Natur Rev. Cancer* **2006**, *6*, 714–727.

(6) Harley, C. B. Telomerase and cancer therapeutics. *Nature Rev. Cancer* **2008**, *8*, 167–179.

(7) Kelland, L. Targeting the Limitless Replicative Potential of Cancer: The Telomerase/Telomere Pathway. *Clin. Cancer Res.* **2007**, *13*, 4960–4963.

(8) (a) Cohen, S. B.; Graham, M. E.; Lovrecz, G. O.; Bache, N.; Robinson, P. J.; Reddel, R. R. A Protein Composition of Catalytically Active Human Telomerase from Immortal Cells. *Science* **2007**, *315*, 1850–1853. (b) Gillis, A. J.; Schuller, A. P.; Skordalakes, E. Structure of the *Tribolium castaneum* telomerase catalytic subunit TERT. *Nature* **2008**, *455*, 633–638.

(9) (a) Chang, J. T.; Chen, Y.; Yang, H.; Chem, C.; Cheng, A. Differential regulation of telomerase activity by six telomerase subunits. *FEBS J.* **2002**, *269*, 3442–3450. (b) Latrick, C. M.; Cech, T. R. POT1-TPP1 enhances telomerase processivity by slowing primer dissociation and aiding translocation. *EMBO J.* **2010**, *29*, 1–10.

(10) Bryan, T. M.; Goodrich, K. J.; Cech, T. R. *Tetrahymena* Telomerase Is Active as a Monomer. *Mol. Biol. Cell* **2003**, *14*, 4794–4804.

(11) (a) Autexier, C.; Lue, N. F. The Structure and Function of Telomerase Reverse Transcriptase. *Annu. Rev. Biochem.* **2006**, *75*, 493–517. (b) Bryan, T. M.; Sperger, J. M.; Chapman, K. B.; Cech, T. R. Telomerase reverse transcriptase genes identified in *Tetrahymena thermophila* and *Oxytricha trifallax*. *Proc. Natl. Acad. Sci. U.S.A.* **1998**, *95*, 8479–8484.

(12) Barma, D. K.; Elayadi, A.; Falck, J. R.; Corey, D. R. Inhibition of Telomerase by BIBR 1532 and related Analogues. *Bioorg. Med. Chem. Lett.* **2003**, *13*, 1333–1336.

(13) Reed, J.; Gunaratnam, M.; Beltran, M.; Reska, A.; Vilar, R.; Neidle, S. TRAP-LIG, a modified telomere repeat amplification protocol assay to quantitate telomerase inhibition by small molecules. *Anal. Biochem.* **2008**, *380*, 99–105.

(14) (a) for β-R, see Ueno, T.; Takahashi, H.; Oda, M.; Mizunuma, M.; Yokoyama, A.; Goto, Y.; Mizushina, Y.; Sakaguchi, K.; Hayashi, H. Inhibition of Human Telomerase of Rubromycins: Implication of Spiroketal System of the Compounds as an Active Moiety. *Biochemistry* **2000**, *39*, 5995–6002. (b) for BIBR, see (i) Pascolo, E; Wenz, C.; Linger, J.; Hauel, N.; Priepk, H.; Kauffman, I.; Garin-Chasa, P.; Rettig, W. J.; Damm, K.; SchnVapp, A. Mechanism of Human Telomerase Inhibition by BIBR1532, a Synthetic, Non-nucleosidedic Drug Candidate. *J. Biol. Chem.* **2002**, *277*, 15566–15572. (ii) Damm, K.; Hemmann, U.; Garin-Chesa, P.; Hauel, N.; Kauffman, I.; Priepke, H.; Niestroj, C.; Daiber, C.; Enenkel, B.; Guilliard, B.; Lauritsch, I.; Muller, E.; Pascolo, E.; Sauter, G.; Pantic, M.; Martens, U. M.; Wenz, C.; Linger, J.; Kraut, N.; Rettig, W. J.; Schnapp, A. A highly selective telomerase inhibitor limiting human cancer cell proliferation. *EMBO J.* **2001**, *20*, 6958–6968. (iii) Wu, K.; Wilkinson, S.; Reich, N. O.; Pettus, T. R. R. Facile Synthesis of Naphthoquinone Spiroketals by Diastereoselective Oxidative [3 + 2] Cycloaddition. *Org. Lett.* **2007**, *9*, 5537–5540. (iv) Protrowska, K.; Kleideiter, E.; Murdter, T. E.; Taetz, S.; Baldes, C.; Schaefer, U.; Lehr, C.; Klotz, U. Optimization of the TRAP assay to evaluate specificity of telomerase inhibitors. *Lab. Invest.* **2005**, *85*, 1565–1569. (v) Also see

ref 12. (c) for THyF, see Menichincheri, M; Ballinary, D.; Bargiotti, A.; Bonomini, L.; Ceccarelli, W.; D'Alessio, R.; Fretta, A.; Moll, J.; Polucci, P.; Soncini, C.; Tibolla, M.; Trosset, J.; Vanotti, E. Catecholic Flavonoids Acting as Telomerase Inhibitors. *J. Med. Chem.* **2004**, *47*, 6466−6475. (d) for EGCG, see Nassani, I.; Seimiya, H.; Tsuruo, T. Telomerase Inhibition, Telomere Shortening, and Senscence of Cancer Cells by Tea Catechins. *Biochem. Biophys. Res. Commun.* **1998**, *249*, 391−396. (e) for MST-312, see (i) Seimiya, H.; Oh-hara, T.; Suzuki, T.; Naasani, I; Shimazaki, T.; Tsuchiya, K.; Tsuruo, T. Telomere Shortening and Growth Inhibition of Human Cancer Cells by Novel Synthetic Telomerase Inhibitors MST-312, MST-295, and MST-199. *Mol. Cancer Ther.* **2002**, *1*, 657−665. (ii) Sigma-Aldrich. (f) TMPyP4, see (i) De Cian, A.; Cristofari, G.; Reichenback, R.; De Lemos, E.; Monchaud, D.; Teulade-Fichou, M.; Shin-ya, K.; Lacroix, L.; Lingner, J.; Mergny, J. Reevaluation of telomerase inhibition by quadruplex ligands and their mechanisms of action. *Proc. Natl. Acad. Sci. U.S.A.* **2007**, *104*, 17347−17352. (ii) Shi, D.; Wheelhouse, R. T.; Sun, D.; Hurley, L. H. Quadruplex-Interactive Agents as Telomerase Inhibitors: Synthesis of Porphyrins and Structure−Activity Relationship for the Inhibition of Telomerase. *J. Med. Chem.* **2001**, *44*, 4509−4523. (iii) Zhang, L.; Huang, J.; Ren, L.; Bai, M.; Wu, L.; Zhai, B.; Zhou, X. Synthesis and evaluation of cationic phthalocyanine derivatives as potential inhibitors of telomerase. *Bioorg. Med. Chem.* **2008**, *16*, 303−312. (iv) Yao, Y.; Wang, Q.; Hao, Y.; Tan, Z. An exonuclease I hydrolysis assay for evaluating G-quadruplex stabilization by small molecules. *Nucleic Acids Res.* **2007**, *35*, e68. (v) Also see ref 13.

(15) (a) Burger, A. M.; Dai, F.; Schultes, C. M.; Reszka, A. P.; Moore, M. J.; Double, J. A.; Neidle, S. The G-Quadruplex-Interactive Molecule BRACO-19 Inhibits Tumor Growth, Consistent with Telomere Targeting and Interference with Telomerase Function. *Cancer Res.* **2005**, *65*, 1489−1496. (B) Kim, M.-Y.; Gleason-Guzman, M.; Izbicka, E.; Nishioka, D.; Hurley, L. H. The Different Biological Effects of Telomestatin and TMPyP4 Can Be Attributed to Their Selectivity for Interaction with Intramolecular or Intermolecular G-Quadruplex Structures. *Cancer Res.* **2003**, *63*, 3247−3256.

(16) Saldanha, S. N.; Andrews, L. G.; Tellefsbol, T. O. Analysis of telomerase activity and detection of its catalytic subunit, hTERT. *Anal. Biochem.* **2003**, *315*, 1−21.

(17) Kim, N. W.; Wu, F. Advances in quantification and characterization of telomerase activity by the telomeric repeat amplification protocol (TRAP). *Nucleic Acids Res.* **1997**, *25*, 2595−2597.

(18) For tetrahymena buffer conditions, see Licht, J. D.; Collins, K. Telomerase RNA function in recombinant *Tetrahymena* telomerase. *Genes Dev.* **1999**, *13*, 1116−1125.

(19) Han, F. X.; Wheelhouse, R. T.; Hurley, L. H. Interactions of TMPyP4 and TMPyP2 with Quadruplex DNA. Structural Basis for the Differential Effects on Telomerase Inhibition. *J. Am. Chem. Soc.* **1999**, *121*, 3561−3570.

(20) Wie, M.; Wynn, R.; Hollis, G.; Liao, B.; Margulis, A.; Reid, B. G.; Klabe, R.; Liu, P. C. C.; Becker-Pasha, M.; Rupar, M.; Burn, T. C.; McCall, D. E.; Li, Y. High-Throughput Determination of Mode of Inhibition in Lead Identification and Optimization. *J. Biomol. Screening* **2007**, *12*, 220−228.

(21) Koshland, D. E.; Nemethy, G.; Filmer, D. Comparison of Experimental Binding Data and Theoretical Models in Proteins Containing Subunits. *Biochemistry* **1966**, *5*, 365−385.

(22) Segel, I. H. *Enzyme Kinetics: Behavior and Analysis of Rapid Equilibrium and Steady State Enzyme Systems*; Wiley Interscience Publication: New York, 1975, pp 176 and 387.

(23) (a) Wenz, C.; Enenkel, B.; Amacker, M.; Kelleher, C.; Damm, K.; Lingner, J. Human telomerase contains two cooperating telomerase RNA molecules. *EMBO J.* **2001**, *20*, 3526−3534. (b) Prescott, J.; Blackburn, E. H. Functionally interacting telomerase RNAs in the yeast telomerase complex. *Genes Dev.* **1997**, *11*, 2790−2800.